nature neuroscience

The organization of two new cortical interneuronal circuits

Xiaolong Jiang[1,4], Guangfu Wang[1,4], Alice J Lee[1,2], Ruth L Stornetta[1] & J Julius Zhu[1,3]

Deciphering the interneuronal circuitry is central to understanding brain functions, yet it remains a challenging task in neurobiology. Using simultaneous quadruple-octuple *in vitro* and dual *in vivo* whole-cell recordings, we found two previously unknown interneuronal circuits that link cortical layer 1–3 (L1–3) interneurons and L5 pyramidal neurons in the rat neocortex. L1 single-bouquet cells (SBCs) preferentially formed unidirectional inhibitory connections on L2/3 interneurons that inhibited the entire dendritic-somato-axonal axis of ~1% of L5 pyramidal neurons located in the same column. In contrast, L1 elongated neurogliaform cells (ENGCs) frequently formed mutual inhibitory and electric connections with L2/3 interneurons, and these L1-3 interneurons inhibited the distal apical dendrite of >60% of L5 pyramidal neurons across multiple columns. Functionally, SBC→L2/3 interneuron→L5 pyramidal neuronal circuits disinhibited and ENGC↔L2/3 interneuron→L5 pyramidal neuronal circuits inhibited the initiation of dendritic complex spikes in L5 pyramidal neurons. As dendritic complex spikes can serve coincidence detection, these cortical interneuronal circuits may be essential for salience selection.

The cerebral cortex is capable of performing multifaceted high-level cognitive tasks, a capability that is believed to reside in the intricate cortical network that contains a diversity of cellular constituents, including a number of distinct inhibitory interneurons[1–6]. However, exactly how the cortical interneuronal circuits are structured to carry out cortical functions remains elusive, largely because of the difficulty of deciphering complex neuronal circuits, a process requiring analysis of multi- or trans-synaptic connections and identification of cell types of many different interconnected interneurons and pyramidal neurons[7–9]. To facilitate the dissection of cortical interneuronal circuits, we developed a stable multiple (up to octuple) whole-cell recording technology that allows the recovery of the detailed morphology of >85% of recorded interneurons and >99% of recorded pyramidal neurons. Using this technology, we were able to decode complex transynaptic interneuronal circuits in acute rat sensorimotor cortex slices.

L1 is likely involved in selection of attentional and salient signals, as it receives inputs primarily from higher order thalamic relays and higher order cortical areas[10–13]. It has been shown that neurons in these thalamic relays and cortical areas preferentially increase their activity during attention-demanding processes (for example, attentional, expectational, perceptual and working memory tasks), and physiological or pharmacological manipulation of the activity of the neurons interferes with attentional tasks[14–17]. Strategically located in L1 are sparsely distributed GABAergic interneurons that belong to two general groups: one group has a heterogeneous morphological appearance and an axon projecting to deeper layers, whereas the others are multipolar, aspiny neurons resembling neurogliaform cells (NGCs) with an axon ramifying densely in L1 (refs. 18–21). *In vivo* recordings have shown that L1 inputs generate direct, rapid excitatory postsynaptic potentials (EPSPs) in L1 interneurons, as well as in apical dendrites of pyramidal neurons in deep layers[19,22], and that the excitation is selectively and markedly enhanced during attentional tasks[23,24]. In L5 pyramidal neurons, near-synchronous L1 modulatory and L4 sensory inputs can serve as a coincidence detection mechanism by inducing dendritic complex spikes and bursts of somatic/axonal action potentials[22,25], which secure the further processing of the signals[26,27]. L1 interneurons can convert L1 inputs into inhibition to mold dendritic integration in pyramidal neurons[18–20,28,29]. However, whether L1 neurons may participate in more complex interneuronal circuits and what these circuits do remains unclear.

We identified two previously unknown and distinct cortical interneuronal circuits that link input-receiving L1 interneurons via L2/3 interneurons to output-producing L5 pyramidal neurons in the rat sensorimotor cortex. One circuit involved a specific type of L1 neuron, the SBCs, which typically formed unidirectional inhibitory connections with all seven types of L2/3 interneurons, and these L2/3 interneurons inhibited the entire dendritic-somato-axonal initial segment axis of a very small number of L5 pyramidal neurons located in the same column. Thus, SBC→L2/3 interneuron→L5 pyramidal neuronal circuits effectively enhanced dendritic complex spiking in L5 pyramidal neurons using a disynaptic disinhibitory mechanism. In contrast, the other circuit involved a different type of L1 neuron, the ENGCs, which frequently formed reciprocal inhibitory and electric connections with three selective types of L2/3 interneurons, and these L1 and L2/3 interneurons inhibited the distal apical dendrite of the majority of L5 pyramidal neurons in the same and neighboring columns. Thus, ENGC↔L2/3 interneuron→L5 pyramidal neuronal circuits powerfully suppressed dendritic complex spiking in L5 pyramidal neurons using a mutual inhibition- and electric coupling–mediated synchronizing mechanism. Beyond converting L1 inputs into inhibition, these two distinct interneuronal circuits were

[1]Department of Pharmacology, School of Medicine, University of Virginia, Charlottesville, Virginia, USA. [2]Department of Biology, College of Arts and Sciences, University of Virginia, Charlottesville, Virginia, USA. [3]Department of Neuroscience, School of Medicine, University of Virginia, Charlottesville, Virginia, USA. [4]These authors contributed equally to this work. Correspondence should be addressed to J.J.Z. (jjzhu@virginia.edu).

Received 18 June 2012; accepted 5 December 2012; published online 13 January 2013; corrected after print 3 March 2013; doi:10.1038/nn.3305

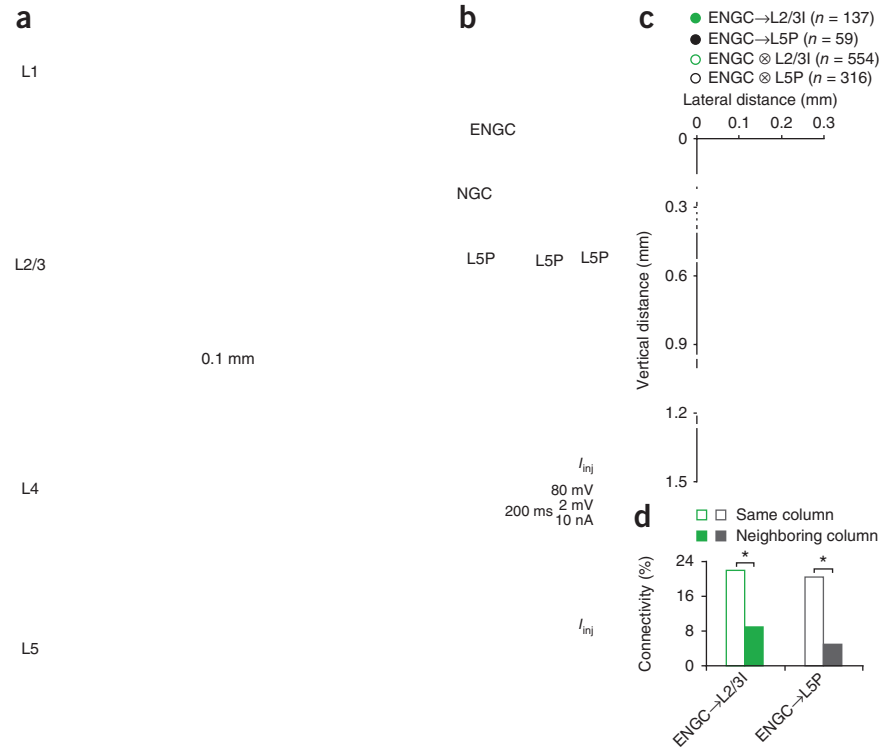

Figure 4 ENGCs form inhibitory circuits across multiple columns. (**a**) Reconstruction of L1 ENGC (green), L2 NGC (brown) and multiple L5 pyramidal neurons recorded simultaneously. The double colored dots indicate the putative synaptic contacts. Note the putative synaptic contacts from ENGC on terminal tuft dendrites of L5 pyramidal neurons. (**b**) Single action potentials elicited in presynaptic ENGC and NGC evoked uIPSPs in postsynaptic NGC, ENGC and two L5 pyramidal neurons (gray and black). The schematic shows the synaptic connections. Scale bars apply to all recording traces with 80 mV and 2 mV bars applied to traces with and without action potentials, respectively. (**c**) The plot shows the relative position of L2/3 interneurons and L5 pyramidal neurons to ENGCs and connectivity between ENGCs and L2/3 interneurons or L5 pyramidal neurons in the same and neighboring columns. Note the origin of *x* and *y* axes indicating the soma location of ENGCs, filled and empty dots representing connected and unconnected neurons, respectively, and reduced cell density at the border of columns. (**d**) Values for the connectivity of ENGC→L2/3I (ENGC→L2/3I$_{Same\ column}$, 22.1%, $n = 126$ of 570 tested connections; ENGC→L2/3I$_{Neighboring\ column}$, 9.1%, $n = 11$ of 121 tested connections; $\chi^2 = 10.6$) and ENGC→L5P (ENGC→L5P$_{Same\ column}$, 20.4%, $n = 53$ of 259 tested connections; ENGC→L5P$_{Neighboring\ column}$, 5.2%, $n = 6$ of 116 tested connections; $\chi^2 = 14.1$) are shown. $^*P < 0.05$ (χ^2 tests).

ENGCs had similar axonal arborizations, but differed in somatodendritic properties (**Supplementary Fig. 4**). In particular, MaCs, NGCs and BTCs postsynaptic to SBCs were located throughout the entire L2/3 with <10% of their dendritic arborization found in L1. In contrast, MaCs, NGCs and BTCs postsynaptic to ENGCs were located in the upper half of L2/3 with ~50% of their dendritic arborization positioned in L1 (**Supplementary Fig. 4**). Collectively, these anatomical, physiological and pharmacological results indicate that SBCs and ENGCs form two anatomically and functionally distinct interneuronal circuits: SBC→ and ENGC↔L2/3 interneuronal circuits.

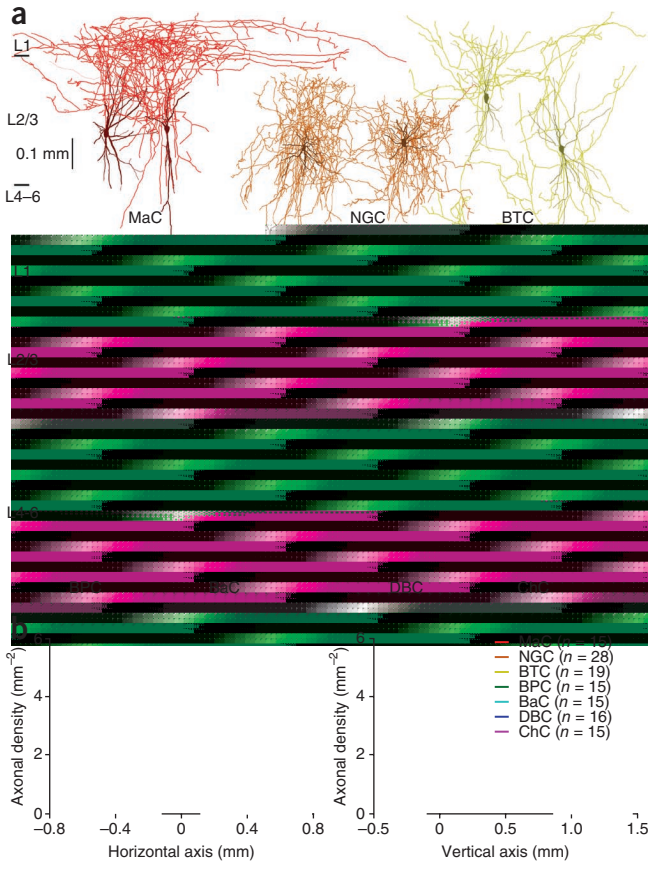

Figure 5 L2/3 interneurons exhibit distinctive axonal arborization patterns. (**a**) Reconstruction of two MaCs (red), two NGCs (brown), two BTCs (dark yellow-green), two BPCs (dark green), two BaCs (cyan), two DBCs (blue) and two ChCs (purple) recorded in L2/3 of acute cortical slices. (**b**) Axonal length density plots show significant differences in axonal density at both the horizontal and vertical axes of L2/3 interneurons (MaC, $n = 15$; NGC, $n = 28$; BTCs, $n = 19$; BPC, $n = 15$; BaC, $n = 15$; DBC, $n = 16$; ChC, $n = 15$; $F > 185$, $P < 0.001$, ANOVA tests). Note the origin of *x* and *y* axes indicating the soma location of interneurons and positive direction of the vertical axis pointing to the cortical white matter. Error bars represent s.e.m.

Interneuronal circuits differentially target L5 neurons

We then examined excitatory postsynaptic neurons targeted by SBC→ and ENGC↔L2/3 interneuronal circuits, focusing primarily on L5 pyramidal neurons, the major cortical output neurons (**Figs. 3** and **4** and **Supplementary Fig. 5**). Simultaneous whole-cell recordings from multiple L1–3 interneurons and L5 pyramidal neurons revealed that SBCs did not directly inhibit L5 pyramidal neurons (**Fig. 3** and **Supplementary Fig. 5**). Instead, L2/3 interneurons postsynaptic to SBCs inhibited ~9% of L5 pyramidal neurons located in the same columns, but these L2/3 interneurons did not inhibit L5 pyramidal neurons in neighboring columns (**Fig. 3c,d** and **Supplementary Fig. 5**). In contrast, ENGCs directly inhibited ~20% of L5 pyramidal neurons recorded in the same columns and they also directly inhibited ~5% of L5 pyramidal neurons recorded in neighboring columns (**Fig. 4**). In addition, L2/3 interneurons postsynaptic to ENGCs inhibited

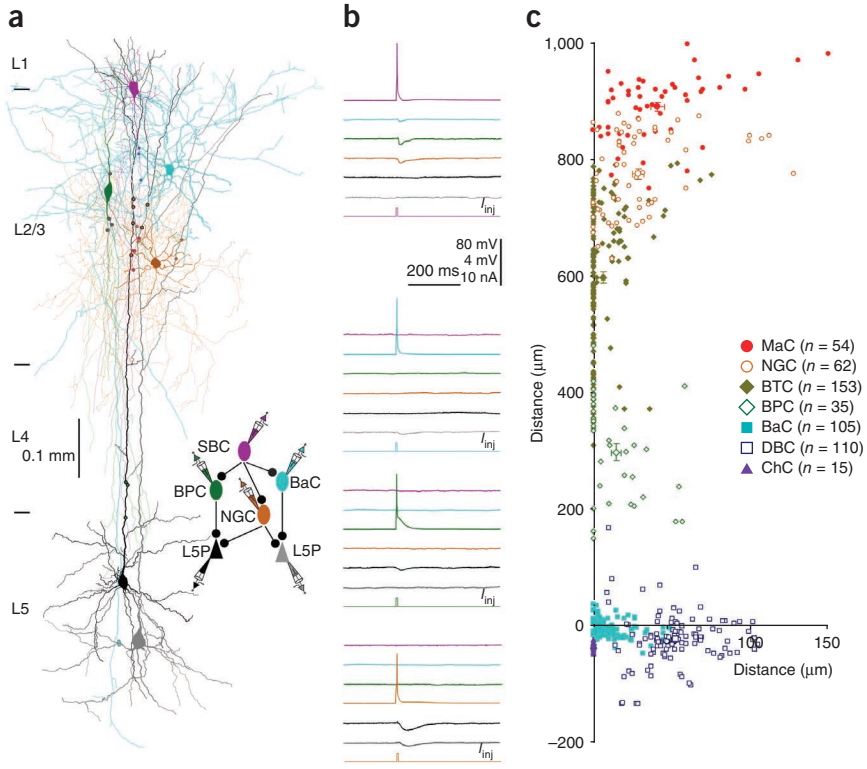

Figure 6 L2/3 interneurons target different compartments of L5 pyramidal neurons. (**a**) Reconstruction of L1 SBC (magenta), L2/3 NGC (brown), L2/3 BPC (dark green), L2/3 BaC (cyan) and two L5 pyramidal neurons (black and gray) recorded simultaneously from an acute cortical slice. The double colored dots indicate the putative synaptic contacts. (**b**) Single action potentials elicited in presynaptic SBC, NGC, BPC and BaC evoked uIPSPs in postsynaptic NGC, BPC, BaC and L5 pyramidal neurons, respectively. The schematic shows the synaptic connections. Scale bars apply to all recording traces with 80 mV and 4 mV bars applied to traces with and without action potentials, respectively. (**c**) The coordinates, or the horizontal and vertical distance of the synapses made by seven groups of L2/3 interneurons from the soma of L5 pyramidal neurons (MaC, lateral = 41.2 ± 4.3 μm, vertical = 890.3 ± 7.4 μm, n = 54 from 10 MaCs; NGC, lateral = 28.8 ± 3.8 μm, vertical = 774.3 ± 8.6 μm, n = 62 from 17 NGCs; BTC, lateral = 6.5 ± 1.1 μm, vertical = 597.3 ± 9.9 μm, n = 153 from 27 BTCs; BPC, lateral = 14.5 ± 3.2 μm, vertical = 299.5 ± 14.4 μm, n = 35 from 8 BPCs; BaC, lateral = 11.8 ± 1.2 μm, vertical = –0.6 ± 1.5 μm, n = 105 from 28 BaCs; DBC, lateral = 53.0 ± 2.2 μm, vertical = –19.2 ± 4.3 μm, n = 110 from 26 DBCs; ChC, lateral = 0.0 ± 0.0 μm, vertical = –30.6 ± 1.6 μm, n = 15 from 4 ChCs). The coordinates not shown ($MaC_{\leftarrow ENGC}$, lateral = 41.6 ± 7.5 μm, vertical = 898.2 ± 8.3 μm, n = 14 from 3 MaCs; $NGC_{\leftarrow ENGC}$, lateral = 32.1 ± 5.3 μm, vertical = 783.6 ± 11.5 μm, n = 38 from 11 NGCs; $BTC_{\leftarrow ENGC}$, lateral = 8.0 ± 1.8 μm, vertical = 601.8 ± 24.0 μm, n = 38 from 7 BTC; ENGC, lateral = 70.8 ± 7.6 μm, vertical = 937.2 ± 5.1 μm, n = 27 from 6 ENGCs).

~20% of L5 pyramidal neurons in the same column (**Fig. 4c**,**d** and **Supplementary Fig. 5**). Together, these results suggest that SBCs form disynaptic disinhibitory connections with L5 pyramidal neurons via L2/3 interneurons in single columns, whereas interconnected ENGCs and L2/3 interneurons form direct inhibitory connections with L5 pyramidal neurons in the same and/or neighboring columns.

To determine whether distinct L2/3 interneurons may be differentially involved in SBC→ and ENGC↔L2/3 interneuron→L5 pyramidal neuronal circuits, we further analyzed the inhibitory synaptic connections formed between distinct L2/3 interneurons and L5 pyramidal neurons. Notably, light microscopic examination revealed that each of seven types of L2/3 interneurons contacted a specific, largely non-overlapping subcellular compartment of L5 pyramidal neurons with multiple synaptic boutons and, together, they subdivided the entire membrane surface of the dendritic-somato-axonal initial segment region (**Fig. 6** and **Supplementary Table 2**). Specifically, the synaptic boutons of MaCs were on terminal tuft dendrites, those of NGCs were on secondary and tertiary tuft dendrites, those of BTCs were on distal dendritic trunks and primary tuft dendrites, those of BPCs were on middle dendritic trunks and oblique dendrites, those of BaCs were on somata and proximal dendrites, those of DBCs were on middle and distal basal dendrites, and those of ChCs were on axonal initial segments of L5 pyramidal neurons. At times, we recorded two (n = 16) or three (n = 4) distinct L2/3 interneurons innervating the same postsynaptic L5 pyramidal neurons, and morphological reconstruction showed that the synapses from distinct L2/3 interneurons did not intermingle in their target areas of L5 pyramidal neurons (**Fig. 6a**,**b**). Subsequent electron microscopic serial section examination confirmed that the majority of light microscopically identified synaptic boutons were actual synapses (~80%, n = 69 of 89 boutons from 15 interneurons) with symmetric membrane densities (**Supplementary Fig. 6** and **Supplementary Table 2**), consistent with the notion that light microscopically identified synaptic boutons are reliable indicators of synapses[30,31]. Collectively, these results suggest that L1–3 interneurons form distinct interneuronal circuits; that is, SBC→ and ENGC↔L2/3 interneuron→L5 pyramidal neuronal circuits differentially control distinct subcellular compartments of L5 pyramidal neurons.

Interneuronal circuits regulate dendritic complex spiking

To determine the possible functional roles of SBC→ and ENGC↔L2/3 interneuron→L5 pyramidal neuronal circuits, which seem to target multiple distinct dendritic-somato-axonal compartments in L5 pyramidal neurons[27,32–34], we examined their effects on dendritic and somatic spiking (**Fig. 7**). As with previous reports[22,25], simultaneously injecting currents in the shape of an EPSP at the dendrite and soma of L5 pyramidal neurons evoked a dendritic complex spike and a burst of two to three somatic action potentials in the neurons (**Fig. 7b**,**e**). The dendritic complex spikes consisted of a sequence of events, including an initial soma/axon-initiated back-propagating action potential, followed by a dendrite-initiated slow action potential and an additional one or more soma/axon-initiated action potential(s) (**Fig. 7b**), indicative of an interaction between somatic/axonal and dendritic action potential zones[25]. Depolarizing L2/3 interneurons in either SBC→ or ENGC↔L2/3 interneuron→L5 pyramidal neuronal circuits with continuous current injection elicited tonic firing of single action potentials in interneurons, which induced uIPSPs in the dendrite and soma of L5 pyramidal neurons, and suppressed complex dendritic spiking and somatic bursting in L5 pyramidal neurons (**Fig. 7c**,**e**), consistent with previous findings[25]. Notably, action potentials in SBCs evoked by short depolarizing pulses effectively abolished the depolarization-elicited firing in all L2/3 interneurons, blocked L2/3 interneuron–mediated uIPSPs, and reversed the suppression of

complex dendritic spiking and somatic bursting in L5 pyramidal neurons ($n = 9$ neurons; **Fig. 7d**,**e**). There was a slight increase in incidence of dendritic complex spikes after current injection in both SBCs and their postsynaptic L2/3 interneurons (**Fig. 7e**), suggesting that additional L2/3 interneurons of the same disynaptic circuits are located in the same compact columnar areas (**Fig. 3**). In sharp contrast, short pulse–evoked action potentials in ENGCs consistently synchronized the depolarization-elicited tonic firing in all L2/3 interneurons, potentiated L2/3 interneuron–mediated uIPSPs, and enhanced the suppression of complex dendritic spiking and somatic bursting in L5 pyramidal neurons ($n = 10$ neurons; **Fig. 7d**,**e**). These results suggest that activation of SBC→L2/3 interneuronal circuits disinhibits and activation of ENGC↔L2/3 interneuronal circuits inhibits the initiation of complex dendritic spikes in L5 pyramidal neurons.

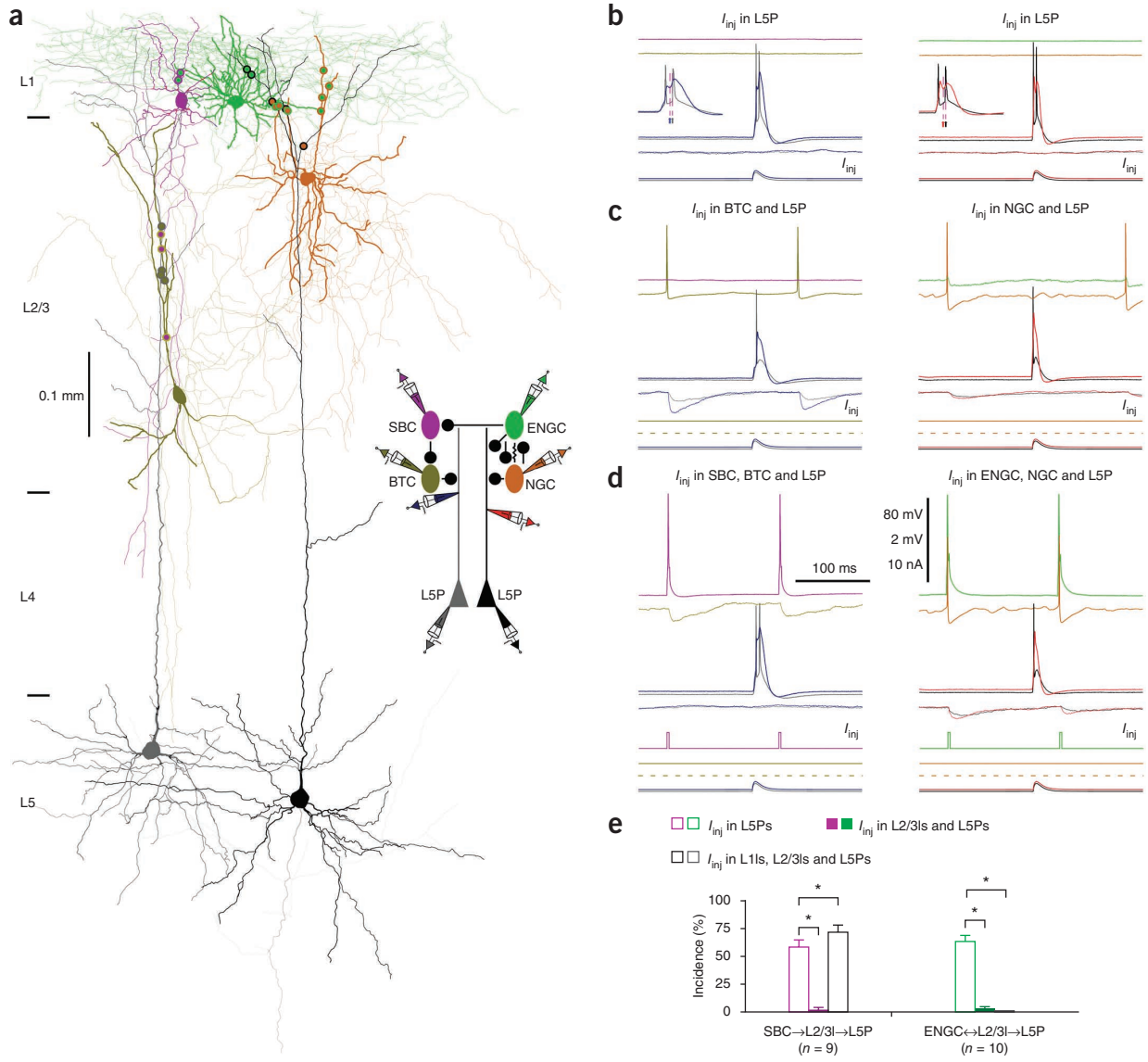

Figure 7 SBC→ and ENGC↔L2/3I→L5 pyramidal neuronal circuits serve different functions. (**a**) Reconstruction of L1–3 interneurons and L5 pyramidal neurons recorded simultaneously from an acute cortical slice. The double colored dots indicate the putative synaptic contacts. The schematic shows the synaptic connections and dendritic recording sites. (**b**–**d**) The effects of continuous (in L1 interneurons) or brief (in L2/3 interneurons) depolarizing current injections on the dendritic complex spikes evoked by simultaneous near-threshold current injections from the dendritic and somatic recording electrodes in the shape of an EPSP. Scale bars apply to all recording traces in **b**–**d** with 80 mV and 2 mV bars applied to traces with and without action potentials, respectively. Note the reduced number of somatic action potentials after activation of L2/3 interneurons (N_{Before}, 2.3 ± 0.1; N_{After}, 1.0 ± 0.0; $n = 19$, $Z = 4.0$, $P < 0.005$, Wilcoxon test) and NGC firing-evoked spikelets in ENGC. Insets in **b** show the sequences of soma/axon–dendrite–soma/axon-initiated events in the dendritic complex spikes at a timescale expanded by a factor of 2.5; arrows indicate the timing of initiation of the dendritic slow potentials and second somatic action potentials. (**e**) The incidences of dendritic complex spikes after current injections in L1–3 interneurons. Values for the incidences in SBC (I_{inj} in L5P, 56.9 ± 6.6%; I_{inj} in L2/3I and L5P, 1.4 ± 1.3%; $Z = 2.7$; I_{inj} in SBC, L2/3I and L5P, 70.8 ± 6.3%; $Z = 2.0$, $n = 9$) and ENGC (I_{inj} in L5P, 62.5 ± 5.3%; I_{inj} in ENGC and L5P, 13.8 ± 5.1%; $Z = 2.9$; I_{inj} in L2/3I and L5P, $Z = 2.8$, 2.5 ± 1.7%; I_{inj} in ENGC, L2/3I and L5P, 0.0 ± 0.0%, $Z = 2.8$; $n = 10$) interneuronal circuits are shown. Note that larger uIPSPs were induced by the synchronized firing in ENGCs and their targeting L2/3 interneurons (recorded in L5 pyramidal neurons at resting membrane potentials) (ENGC↔L2/3I: 0.55 ± 0.07 mV; ENGC: 0.25 ± 0.04 mV; $Z = 2.8$; L2/3I: 0.33 ± 0.05 mV; $Z = 2.8$; $n = 10$, $P < 0.01$, Wilcoxon tests). *$P < 0.05$ (Wilcoxon tests). Error bars represent s.e.m.

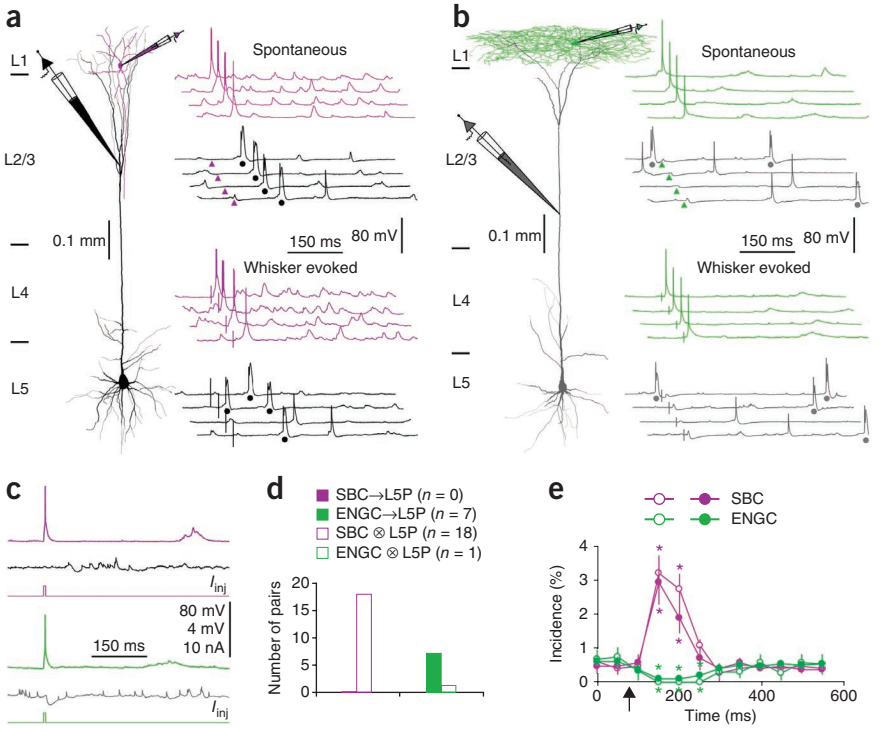

Figure 8 SBC→ and ENGC↔L2/3I→L5 pyramidal neuronal circuits differ in function *in vivo*. (**a**,**b**) Reconstruction of L1 SBC (magenta) or L1 ENGC (green) and L5 pyramidal neurons (black or gray) recorded simultaneously in intact animals. Note that the recording traces are aligned by spontaneous somatic action potentials or whisker stimulation, and arrowheads indicate the time of initiation of spontaneous somatic action potentials in simultaneously recorded L1 interneurons and dots indicate the dendritic complex spikes in L5 pyramidal neurons. (**c**) The average traces revealed that the firing in a SBC promoted and that in an ENGC suppressed the initiation of dendritic complex spikes (appeared as spikelet-like events as a result of averaging) recorded in L5 pyramidal neurons. Scale bars in **a**–**c** apply to all recording traces with 80 mV and 4 mV bars applying to traces with and without action potentials, respectively. (**d**) Connectivity of synapses formed by SBCs and ENGCs on L5 pyramidal neurons recorded simultaneously in intact brains (SBC→L5P, 0.0%, $n = 0$ of 18 tested connections; ENGC→L5P, 85.7%, $n = 7$ of 8 tested connections; $\chi^2 = 21.6$, $P < 0.005$, χ^2 tests). (**e**) Time course of SBC-induced promotion ($n = 3$) and ENGC-induced suppression ($n = 7$) of dendritic complex spiking in L5 pyramidal neurons. Note the SBC- and ENGC-mediated spontaneous and whisker-evoked effects (open dots) and current pulse-evoked effects (filled dots), and the time of somatic action potential initiation in L1 interneurons (indicated by the upward arrow). Note that ENGC-mediated $GABA_B$ responses, although small, were effective in inducing a prolonged suppression of dendritic complex spiking, consistent with employment of a calcium conductance-suppression mechanism[50]. $^*P < 0.05$ ($U = 0.0$, Mann-Whitney rank sum tests). Error bars represent s.e.m.

To confirm the functions of SBC→ and ENGC↔L2/3 interneuron→L5 pyramidal neuronal circuits in intact brains, we made simultaneous dual recordings from SBCs or ENGCs and L5 pyramidal neurons *in vivo* (**Fig. 8**). Simultaneous somatic recordings from SBCs and dendritic recordings from L5 pyramidal neurons showed numerous spontaneous or whisker-evoked events, which occasionally reached threshold and triggered somatic action potentials in SBCs and dendritic complex spikes in L5 pyramidal neurons. Correlation analysis revealed that, in some paired recordings ($n = 3$ of 18 pairs), initiation of action potentials in SBCs enhanced dendritic complex spiking in L5 pyramidal neurons for ~200 ms (**Fig. 8a**,**e**). To confirm the causal effect, we elicited action potentials in SBCs by directly injecting short depolarizing pulses. The evoked action potentials in SBCs enhanced dendritic complex spiking in L5 pyramidal neurons in the same three paired recordings (**Fig. 8c**,**e**). Consistent with our *in vitro* results, the evoked action potentials in SBCs did not induce uIPSPs in L5 pyramidal neurons ($n = 0$ of 18 pairs; **Fig. 8c**,**d**). Similarly, paired recordings showed that spontaneous and whisker-evoked events sometimes reached threshold and triggered somatic action potentials in ENGCs and dendritic complex spikes in L5 pyramidal neurons. However, in the majority of paired recordings ($n = 7$ of 8 pairs), spontaneous and whisker-evoked action potentials in ENGCs suppressed dendritic complex spiking in L5 pyramidal neurons for ~400 ms (**Fig. 8b**,**e**). In the same seven paired recordings, the short pulse–evoked action potentials in ENGCs induced uIPSPs and blocked dendritic complex spiking in L5 pyramidal neurons (**Fig. 8c**,**e**), suggesting a direct causal effect. Notably, recordings from many ENGCs, but none of the SBCs, displayed spikelet-like events, some of which seemed involved in the initiation of action potentials in ENGCs (**Supplementary Fig. 7**), suggesting a contribution of electric synapses in synchronizing firing in ENGC↔L2/3 interneuronal circuits. Collectively, these *in vitro* and *in vivo* results suggest that SBC→L2/3 interneuron→L5 pyramidal neuronal circuits serve to disinhibit and, in a complementary fashion, ENGC↔L2/3 interneuron→L5 pyramidal neuronal circuits function to inhibit dendritic complex spiking in L5 pyramidal neurons.

DISCUSSION

Here, we deciphered the architecture of two interneuronal circuits that link L1–3 interneurons and L5 pyramidal neurons in the neocortex (**Supplementary Fig. 8**). L1 SBCs preferentially formed unidirectional inhibitory connections with all seven types of L2/3 interneurons and trans-synaptically controlled inhibition along the entire dendritic-somato-axonal axis of a few L5 pyramidal neurons in single columns. In contrast, L1 ENGCs frequently formed mutual inhibitory and electric connections with only three selective types of L2/3 interneurons, and, together, they regulated inhibition at the distal apical dendrite of many pyramidal neurons across multiple columns. Functionally, SBC→L2/3 interneuron→L5 pyramidal neuronal circuits disinhibited and ENGC↔L2/3 interneuron→L5 pyramidal neuronal circuits inhibited the initiation of dendritic complex spikes in L5 pyramidal neurons. Given that dendritic complex spiking can serve as a coincidence detection mechanism[22,25], these two interneuronal circuits may be important for selecting and processing salient information.

Organization of cortical interneuronal circuits

We identified two cortical interneuronal circuits, SBC→ and ENGC↔L2/3 interneurons→L5 pyramidal neuronal circuits, which exhibit distinct architecture (**Supplementary Fig. 8**). Previous *in vitro* and *in vivo* recordings have shown that L1 SBCs fire adapting non–late-spiking action potentials, whereas L1 ENGCs fire non-adapting

late-spiking action potentials[18,19]. However, a recent study reported a few exceptions[21]. We analyzed a large number of L1 interneurons and found that there were actually many exceptions. Thus, instead of relying on firing patterns, we classified L1 interneurons on the basis of their visually distinguishable axonal arborization patterns, which were quantitatively confirmed with axonal length density analysis (**Fig. 1b**), as well as with Sholl and polar analyses (data not shown). Notably, SBCs preferentially formed unidirectional inhibitory circuits with L2/3 interneurons and they produced $GABA_A$ receptor–mediated fast inhibition, whereas ENGCs frequently formed mutual inhibitory and electric circuits with L2/3 interneurons and generated $GABA_A$ and $GABA_B$ receptor–mediated slow inhibition.

SBC→ and ENGC↔L2/3 interneuronal circuits also differed in how they connected with L5 pyramidal neurons (**Supplementary Fig. 8**). L5 pyramidal neurons have two general input-receiving domains, an apical dendritic domain and an oblique/basal dendritic-somato-axonal domain[22,33,35], which receive primarily modulatory and sensory inputs, respectively[13]. Our analysis revealed that seven types of L2/3 interneurons (that is, MaCs, NGCs, BTCs, BPCs, BaCs, DBCs and ChCs) synapsed on different subcellular compartments of L5 pyramidal neurons and, together, their synapses subdivided the entire membrane surface of the dendritic-somato-axonal initial segment region. SBCs controlled both the apical and oblique/basal dendritic domains of L5 pyramidal neurons via inhibition of all seven types of L2/3 interneurons (**Figs. 3** and **7**), whereas ENGCs regulated only the apical dendritic domain of L5 pyramidal neurons via direct inhibition (**Figs. 4** and **7**) or via output synchronization with MaCs, NGCs and BTCs (**Fig. 7**). In particular, SBCs never inhibited L5 pyramidal neurons. Instead, SBCs inhibited 13.0% of L2/3 interneurons, and these L2/3 interneurons inhibited 8.7% of L5 pyramidal neurons in the same columns (**Fig. 3** and **Supplementary Fig. 5**). Thus, we estimate that SBC→L2/3 interneuron→L5 pyramidal neuronal circuits may provide disinhibition on dendritic complex spiking in a small percentage (P = 13.0% × 8.7% ≈ 1%) of disynaptically connected L5 pyramidal neurons. In contrast, ENGCs inhibited 20.4%, and MaC, NGC and BTC L2/3 interneurons postsynaptic to ENGCs inhibited 7.1, 33.3 and 15.8% of L5 pyramidal neurons in the same columns (**Supplementary Fig. 5**). These L1–3 interneurons may fire alone and independently inhibit L5 pyramidal neurons. Alternatively, when activated together, they may fire in synchrony and more effectively inhibit L5 pyramidal neurons (**Fig. 7**). The synchronization of outputs in these interneurons seems dependent on their frequent mutual inhibitory and electrical synapses, as these synapses were able to cooperate (complementarily and synergistically) in synchronizing firing in interneuronal networks, whereas electric gap junctional potentials (or spikelets) promote coinitiation of action potentials when inhibition fades (acting as an excitatory force), and inhibitory synaptic potentials rapidly curtail spikelets and suppress initiation of action potentials during their presence (acting as an inhibitory force)[3,36,37]. Thus, we calculate that ENGC↔L2/3 interneuron→L5 pyramidal neuronal circuits may inhibit the majority (P = 100% − (100 − 20.4%) × (100 − 7.1%) × (100 − 33.3%) × (100 − 15.8%) ≈ 60%) of monosynaptically connected L5 pyramidal neurons located in the same columns alone. Together, these results suggest that SBC→L2/3 interneuron→L5 pyramidal neuronal circuits are structured to disinhibit a small population of L5 pyramidal neurons, whereas ENGC↔L2/3 interneuron→L5 pyramidal neuronal circuits are organized to inhibit a large population of L5 pyramidal neurons.

Functional implications of cortical interneuronal circuits

Our results indicate that SBC→ and ENGC↔L2/3 interneuron→L5 pyramidal neuronal circuits function beyond transforming L1 inputs into inhibition. Instead of suppressing spiking, SBCs enhanced dendritic complex spiking in L5 pyramidal neurons by inhibiting L2/3 interneurons that are spontaneously active in intact brains[24,28,38,39]. Thus, SBC→L2/3 interneuron→L5 pyramidal neuronal circuits use a di-synaptic disinhibitory mechanism to permit the initiation of dendritic complex spikes in a few L5 pyramidal neurons in a small area, which nonlinearly amplifies the selected signals. Conversely, ENGC↔L2/3 interneuron→L5 pyramidal neuronal circuits employ a mutual inhibition- and electric coupling–mediated synchronizing mechanism to synchronize the firing of interneurons. These interneurons can then supply powerful inhibition to suppress dendritic complex spiking in many L5 pyramidal neurons over a broader area, which effectively increases the signal-to-noise ratio by reducing background noise and sharpens the receptive field by suppressing surrounding activity. Moreover, SBCs have a smaller receptive field with higher acuity than ENGCs[19], which may produce a much smaller suprathreshold field[40–42]. Finally, SBCs receive the earliest L1 inputs and they are rapidly inactivated after their initial activation[19], presumably as a result of inhibition from ENGCs[18,20] and from MaCs, NGCs and BTCs targeted by ENGCs (**Supplementary Table 1**). Together, these results suggest that SBC→ and ENGC↔L2/3 interneuron→L5 pyramidal neuronal circuits may work together to select and nonlinearly amplify a very few spatially and temporally defined signals.

We found a few other architectural features of SBC→ and ENGC↔L2/3 interneuron→L5 pyramidal neuronal circuits that may also be important to function. For example, SBCs innervated fewer (<10%) MaCs, NGCs, BaCs and DBCs, but more BTCs (14.6%) and ChCs (17.3%), and many more BPCs (27.9%) (**Supplementary Table 1**). Whereas BTCs and ChCs targeted the dendritic and axonal action potential initiation zones, respectively, BPCs targeted the middle dendritic trunk critical for interaction of the dendritic and axonal action potential initiation zones in L5 pyramidal neurons[22,43]. Thus, we speculate that SBC→L2/3 interneuronal circuits may be particularly effective at controlling the initiation of dendritic complex spikes, which requires the interaction of dendritic and axonal action potentials[25,43]. In addition, although MaCs, NGCs and BTCs involved in different circuits had the same axonal anatomy, they differed in dendritic branching patterns. In particular, MaCs, NGCs and BTCs targeted by ENGCs had their dendrites ramifying extensively into L1 (**Supplementary Fig. 4**), and they may receive direct L1 inputs[11], enabling them to directly convert L1 inputs into inhibition in L5 pyramidal neurons. These results also suggest that MaCs, NGCs and BTCs may be further divided into functional subgroups, which is consistent with other evidence supporting the possibility of functionally subdividing L2/3 interneurons (that is, BaCs and NGCs)[44–46]. One obvious question that remains to be addressed is how distinct groups and/or subgroups of L2/3 interneurons may differentially contribute to cortical functions and whether they alter their activity coordinately and/or independently during different information processing tasks and behavioral states in unanesthetized animals[28,39,47].

We propose that SBC→ and ENGC↔L2/3 interneuron→L5 pyramidal neuronal circuits control the filtering of information, which is supported by several lines of evidence. First, SBC→ and ENGC↔L2/3 interneuron→L5 pyramidal neuronal circuits control the initiation of dendritic complex spikes, which can function as a coincidence detection mechanism to select salient inputs[22,25]. Second, the primary L1 inputs come from feedforward connections from higher order thalamic relays and feedback connections from higher order cortical areas[10–13], and the neuronal activity in these thalamic relays and cortical areas initiates selection of salient information[14,15,17,48]. Third, theoretical and experimental findings suggest that attentional

influence consists of both the signal augmenting and receptive field sharpening processes[15,17]. Consistent with this concept, SBC→L2/3 interneuronal circuits enhanced dendritic complex spiking in a small spatially and temporally restricted population of L5 pyramidal neurons and ENGC↔L2/3 interneuronal circuits suppressed dendritic complex spiking in the majority of L5 pyramidal neurons over a large area, effectively augmenting the signal-to-noise ratio and sharpening the receptive field. Finally, salience selection is central to many attention-demanding high-level cognitive behaviors, and accumulating evidence indicates that a number of neurological, mental and/or psychiatric disorders associated with attention deficits exhibit impairments of interneuronal function (for example, see refs. 15,49).

METHODS

Methods and any associated references are available in the online version of the paper.

Note: Supplementary information is available in the online version of the paper.

ACKNOWLEDGMENTS

We thank E. Callaway, A. Erisir, J. Huang, J. Kapur and G. Tamas for technical advice and invaluable discussions, and members of the Zhu laboratory for comments and technical assistance. This study was supported in part by a postdoctoral fellowship from the Epilepsy Foundation (X.J.), a small research grant from the College of Arts and Sciences of the University of Virginia (A.J.L.) and the US National Institutes of Health.

AUTHOR CONTRIBUTIONS

X.J., G.W. and J.J.Z. designed and developed the mechanics (X.J. and J.J.Z.), electronics and software programs (G.W. and J.J.Z.) for the stable octuple whole-cell recording technology. X.J., G.W., R.L.S. and J.J.Z. developed the immunostaining, neuronal morphology and/or ultrastructural analysis procedures. X.J., G.W., A.J.L. and J.J.Z. performed the experiments and data analysis. X.J., G.W., A.J.L., R.L.S. and J.J.Z. wrote the manuscript.

COMPETING FINANCIAL INTERESTS

The authors declare no competing financial interests.

Published online at http://www.nature.com/doifinder/10.1038/nn.3305.
Reprints and permissions information is available online at http://www.nature.com/reprints/index.html.

1. McBain, C.J. & Fisahn, A. Interneurons unbound. *Nat. Rev. Neurosci.* **2**, 11–23 (2001).
2. Markram, H. *et al.* Interneurons of the neocortical inhibitory system. *Nat. Rev. Neurosci.* **5**, 793–807 (2004).
3. Bartos, M., Vida, I. & Jonas, P. Synaptic mechanisms of synchronized gamma oscillations in inhibitory interneuron networks. *Nat. Rev. Neurosci.* **8**, 45–56 (2007).
4. Ascoli, G.A. *et al.* Petilla terminology: nomenclature of features of GABAergic interneurons of the cerebral cortex. *Nat. Rev. Neurosci.* **9**, 557–568 (2008).
5. Burkhalter, A. Many specialists for suppressing cortical excitation. *Front. Neurosci.* **2**, 155–167 (2008).
6. Klausberger, T. & Somogyi, P. Neuronal diversity and temporal dynamics: the unity of hippocampal circuit operations. *Science* **321**, 53–57 (2008).
7. Luo, L., Callaway, E.M. & Svoboda, K. Genetic dissection of neural circuits. *Neuron* **57**, 634–660 (2008).
8. Brown, S.P. & Hestrin, S. Cell-type identity: a key to unlocking the function of neocortical circuits. *Curr. Opin. Neurobiol.* **19**, 415–421 (2009).
9. Wu, G.K., Tao, H.W. & Zhang, L.I. From elementary synaptic circuits to information processing in primary auditory cortex. *Neurosci. Biobehav. Rev.* **35**, 2094–2104 (2011).
10. Cauller, L.J., Clancy, B. & Connors, B.W. Backward cortical projections to primary somatosensory cortex in rats extend long horizontal axons in layer I. *J. Comp. Neurol.* **390**, 297–310 (1998).
11. Gonchar, Y. & Burkhalter, A. Distinct GABAergic targets of feedforward and feedback connections between lower and higher areas of rat visual cortex. *J. Neurosci.* **23**, 10904–10912 (2003).
12. Rubio-Garrido, P., Perez-de-Manzo, F., Porrero, C., Galazo, M.J. & Clasca, F. Thalamic input to distal apical dendrites in neocortical layer 1 is massive and highly convergent. *Cereb. Cortex* **19**, 2380–2395 (2009).
13. Petreanu, L., Mao, T., Sternson, S.M. & Svoboda, K. The subcellular organization of neocortical excitatory connections. *Nature* **457**, 1142–1145 (2009).
14. Robinson, D.L. & Petersen, S.E. The pulvinar and visual salience. *Trends Neurosci.* **15**, 127–132 (1992).
15. Gilbert, C.D. & Sigman, M. Brain states: top-down influences in sensory processing. *Neuron* **54**, 677–696 (2007).
16. Baluch, F. & Itti, L. Mechanisms of top-down attention. *Trends Neurosci.* **34**, 210–224 (2011).
17. Purushothaman, G., Marion, R., Li, K. & Casagrande, V.A. Gating and control of primary visual cortex by pulvinar. *Nat. Neurosci.* **15**, 905–912 (2012).
18. Chu, Z., Galarreta, M. & Hestrin, S. Synaptic interactions of late-spiking neocortical neurons in layer 1. *J. Neurosci.* **23**, 96–102 (2003).
19. Zhu, Y. & Zhu, J.J. Rapid arrival and integration of ascending sensory information in layer 1 nonpyramidal neurons and tuft dendrites of layer 5 pyramidal neurons of the neocortex. *J. Neurosci.* **24**, 1272–1279 (2004).
20. Wozny, C. & Williams, S.R. Specificity of synaptic connectivity between layer 1 inhibitory interneurons and layer 2/3 pyramidal neurons in the rat neocortex. *Cereb. Cortex* **21**, 1818–1826 (2011).
21. Kubota, Y. *et al.* Selective coexpression of multiple chemical markers defines discrete populations of neocortical GABAergic neurons. *Cereb. Cortex* **21**, 1803–1817 (2011).
22. Larkum, M.E. & Zhu, J.J. Signaling of layer 1 and whisker-evoked Ca^{2+} and Na^{+} action potentials in distal and terminal dendrites of rat neocortical pyramidal neurons *in vitro* and *in vivo*. *J. Neurosci.* **22**, 6991–7005 (2002).
23. Cauller, L.J. & Kulics, A.T. The neural basis of the behaviorally relevant N1 component of the somatosensory-evoked potential in SI cortex of awake monkeys: evidence that backward cortical projections signal conscious touch sensation. *Exp. Brain Res.* **84**, 607–619 (1991).
24. Letzkus, J.J. *et al.* A disinhibitory microcircuit for associative fear learning in the auditory cortex. *Nature* **480**, 331–335 (2011).
25. Larkum, M.E., Zhu, J.J. & Sakmann, B. A new cellular mechanism for coupling inputs arriving at different cortical layers. *Nature* **398**, 338–341 (1999).
26. Lisman, J.E. Bursts as a unit of neural information: making unreliable synapses reliable. *Trends Neurosci.* **20**, 38–43 (1997).
27. Sjöström, P.J., Rancz, E.A., Roth, A. & Hausser, M. Dendritic excitability and synaptic plasticity. *Physiol. Rev.* **88**, 769–840 (2008).
28. Gentet, L.J. *et al.* Unique functional properties of somatostatin-expressing GABAergic neurons in mouse barrel cortex. *Nat. Neurosci.* **15**, 607–612 (2012).
29. Palmer, L.M. *et al.* The cellular basis of $GABA_B$-mediated interhemispheric inhibition. *Science* **335**, 989–993 (2012).
30. Markram, H., Lubke, J., Frotscher, M., Roth, A. & Sakmann, B. Physiology and anatomy of synaptic connections between thick tufted pyramidal neurones in the developing rat neocortex. *J. Physiol. (Lond.)* **500**, 409–440 (1997).
31. Tamás, G., Lorincz, A., Simon, A. & Szabadics, J. Identified sources and targets of slow inhibition in the neocortex. *Science* **299**, 1902–1905 (2003).
32. Reyes, A. Influence of dendritic conductances on the input-output properties of neurons. *Annu. Rev. Neurosci.* **24**, 653–675 (2001).
33. Nevian, T., Larkum, M.E., Polsky, A. & Schiller, J. Properties of basal dendrites of layer 5 pyramidal neurons: a direct patch-clamp recording study. *Nat. Neurosci.* **10**, 206–214 (2007).
34. Larkum, M.E. & Nevian, T. Synaptic clustering by dendritic signaling mechanisms. *Curr. Opin. Neurobiol.* **18**, 321–331 (2008).
35. Antic, S.D. Action potentials in basal and oblique dendrites of rat neocortical pyramidal neurons. *J. Physiol. (Lond.)* **550**, 35–50 (2003).
36. Tamás, G., Buhl, E.H., Lorincz, A. & Somogyi, P. Proximally targeted GABAergic synapses and gap junctions synchronize cortical interneurons. *Nat. Neurosci.* **3**, 366–371 (2000).
37. Kopell, N. & Ermentrout, B. Chemical and electrical synapses perform complementary roles in the synchronization of interneuronal networks. *Proc. Natl. Acad. Sci. USA* **101**, 15482–15487 (2004).
38. Zhu, J.J. & Connors, B.W. Intrinsic firing patterns and whisker-evoked synaptic responses of neurons in the rat barrel cortex. *J. Neurophysiol.* **81**, 1171–1183 (1999).
39. Zhu, Y., Stornetta, R.L. & Zhu, J.J. Chandelier cells control excessive cortical excitation: characteristics of whisker-evoked synaptic responses of layer 2/3 nonpyramidal and pyramidal neurons. *J. Neurosci.* **24**, 5101–5108 (2004).
40. Anderson, J.S., Lampl, I., Gillespie, D.C. & Ferster, D. The contribution of noise to contrast invariance of orientation tuning in cat visual cortex. *Science* **290**, 1968–1972 (2000).
41. Petersen, C.C., Hahn, T.T., Mehta, M., Grinvald, A. & Sakmann, B. Interaction of sensory responses with spontaneous depolarization in layer 2/3 barrel cortex. *Proc. Natl. Acad. Sci. USA* **100**, 13638–13643 (2003).
42. Sun, Y.J. *et al.* Fine-tuning of pre-balanced excitation and inhibition during auditory cortical development. *Nature* **465**, 927–931 (2010).
43. Larkum, M.E., Zhu, J.J. & Sakmann, B. Dendritic mechanisms underlying the coupling of the dendritic with the axonal action potential initiation zone of adult rat layer 5 pyramidal neurons. *J. Physiol. (Lond.)* **533**, 447–466 (2001).
44. Glickfeld, L.L. & Scanziani, M. Distinct timing in the activity of cannabinoid-sensitive and cannabinoid-insensitive basket cells. *Nat. Neurosci.* **9**, 807–815 (2006).
45. Földy, C., Lee, S.Y., Szabadics, J., Neu, A. & Soltesz, I. Cell type–specific gating of perisomatic inhibition by cholecystokinin. *Nat. Neurosci.* **10**, 1128–1130 (2007).
46. Tricoire, L. *et al.* Common origins of hippocampal Ivy and nitric oxide synthase expressing neurogliaform cells. *J. Neurosci.* **30**, 2165–2176 (2010).
47. Adesnik, H., Bruns, W., Taniguchi, H., Huang, Z.J. & Scanziani, M. A neural circuit for spatial summation in visual cortex. *Nature* **490**, 226–231 (2012).
48. Corbetta, M. & Shulman, G.L. Control of goal-directed and stimulus-driven attention in the brain. *Nat. Rev. Neurosci.* **3**, 201–215 (2002).
49. Batista-Brito, R. & Fishell, G. The developmental integration of cortical interneurons into a functional network. *Curr. Top. Dev. Biol.* **87**, 81–118 (2009).
50. Pérez-Garci, E., Gassmann, M., Bettler, B. & Larkum, M.E. The $GABA_{B1b}$ isoform mediates long-lasting inhibition of dendritic Ca^{2+} spikes in layer 5 somatosensory pyramidal neurons. *Neuron* **50**, 603–616 (2006).

ONLINE METHODS

Animal preparation. Young and adult male and female Sprague Dawley rats (≥postnatal, 20 d old), whose cortical inhibitory neurons and circuits are largely mature and relatively stabilized[49,51], were used for *in vitro* (postnatal day 20–41 (P20–41) with ~90% of them to be P20–28, n = 1,104) and *in vivo* (P27–70, n = 172) experiments. All procedures for animal surgery and maintenance were performed following protocols approved by the Animal Care and Use Committee of the University of Virginia and in accordance with US National Institutes of Health guidelines. For *in vitro* experiments, the sensorimotor cortical brain slice preparation followed our previous studies[22,52]. In brief, animals were deeply anesthetized by sodium pentobarbital (90 mg per kg of body weight) and decapitated. The brain was quickly removed and placed into cold (0–4 °C) oxygenated physiological solution containing 125 mM NaCl, 2.5 mM KCl, 1.25 mM NaH_2PO_4, 25 mM $NaHCO_3$, 1 mM $MgCl_2$, 25 mM dextrose and 2 mM $CaCl_2$, pH 7.4. Parasagittal slices (350 μm thick) were cut from the tissue blocks with a microslicer, at an angle (<~4°) closely parallel to apical dendrites of L5 pyramidal neurons, which retained the majority of distal ascending and descending axonal trees of L1–3 interneurons that project into L1 and L5–6. These slices were kept at 37.0 ± 0.5 °C in oxygenated physiological solution for ~0.5–1 h before recordings. During the recording the slices were submerged in a chamber and stabilized with a fine nylon net attached to a platinum ring. The recording chamber was perfused with oxygenated physiological solution containing additional AMPA and NMDA receptor antagonists 20 μM DNQX and 100 μM DL-AP5. The half-time for the bath solution exchange was ~6 s, and the temperature of the bath solution was maintained at 34.0 ± 0.5 °C. All antagonists were bath applied. For *in vivo* experiments, animals were initially anesthetized by an intraperitoneal injection of sodium pentobarbital (60 mg per kg) as previously reported[22,38,39]. Supplemental doses (10 mg per kg) of sodium pentobarbital were given as needed to keep animals free from pain reflexes and in a state of light slow-wave general anesthesia, as determined by monitoring the cortical electroencephalogram, and a relatively steady membrane potential, which were ideal for observing dendritic complex spikes[19,22,38]. All pressure points and incised tissues are infiltrated with bupivacaine. Body temperature (rectal) was monitored and maintained within 37.2 ± 0.3 °C.

Histology and electron microscopy. Light and electron microscopic examinations were carried out following the procedures of our previous reports[22,53]. In brief, after *in vitro* recordings, the slices were fixed by immersion in 3% acrolein/4% paraformaldehyde in 0.1 M phosphate-buffered saline at 4° for 24 h, and then processed with the avidin-biotin-peroxidase method to reveal cell morphology. Some of the slices were subsequently sectioned into 60-μm sections, postfixed in 1% OsO_4, counterstained with 1% uranyl acetate, and flat embedded into resin to carry out electron microscopic examination. The morphologically recovered cells were examined, drawn and analyzed with the aid of a microscope equipped with a computerized reconstruction system Neurolucida (MicroBrightField). Axonal length density plots and maps were calculated per voxel (50 × 50 × 350 μm) using a custom-made program following a previous report[54]. The pyramidal neurons were normalized according to the soma and the main branch point of their apical dendrites[22]. For electron microscopic examination, the small areas of interest (~50 × ~50 μm), each containing putative synaptic boutons from single presynaptic neurons, were embedded in resin, carefully excised and resectioned into 80-nm serial ultrathin sections using an ultramicrotome. No excision and resection was made if synaptic boutons originated from different presynaptic neurons that were too close to be separated. The serial ultrathin sections were examined in sequence with a JEOL-1230 transmission electron microscope (Japan Electron Optic) following the labeled dendrites, which typically led to all light microscopic–identified synapses (except a very few synapses destroyed during electron microscopic processing or hidden behind the grids) at the order predicted by Neurolucida reconstruction. Inhibitory synaptic contacts were determined on the basis of generally accepted criteria[55], including the presence of membranes with parallel alignment forming synaptic clefts that are wider in the middle and close up at one or both edges, the absence of a prominent postsynaptic density, and the presence of multiple flattened synaptic vesicles with at least one docked at the presynaptic membrane.

Electrophysiology. Simultaneous whole-cell *in vitro* and *in vivo* recordings were obtained from cortical neurons as described previously[22,38,39,56]. Briefly, patch recording pipettes (4–7 MΩ) were filled with intracellular solutions containing 135 mM cesium methanesulfonate, 10 mM HEPES, 2.5 mM $MgCl_2$, 4 mM Na_2ATP, 0.4 mM Na_3GTP, 10 mM sodium phosphocreatine, 0.6 mM EGTA, 0.1 mM spermine and 0.5% biocytin (pH 7.25) for current recordings, or 120 mM potassium gluconate, 10 mM HEPES, 4 mM KCl, 4 mM MgATP, 0.3 mM Na_3GTP, 10 mM sodium phosphocreatine and 0.5% biocytin (pH 7.25) for voltage recordings. Whole-cell recordings were made with up to eight Axopatch 200B and/or Axoclamp 2A/B amplifiers (Molecular Devices). To get a relatively unbiased population sample of each type of L2/3 interneuron in cortical slices, we randomly recorded all L2/3 neurons, except pyramidal neurons with an obvious apical dendrite. L5 pyramidal neurons were typically targeted after L1–2/3 interneuronal connections were established. As described previously[22,38,39], *in vivo* dual recordings were targeted to neurons with the same receptive field. Dendritic recordings from L5 pyramidal neurons in intact brain were identified by their characteristic complex spikes, the recording sites were estimated from the distance that the micromanipulator had advanced, taking into account the angle that the electrode formed with the surface of the barrel cortex, and subsequently confirmed with the reconstructed electrode penetration pathways that were revealed after histology processing[38]. An ITC-18 interface board (HEKA Instruments) was custom-modified to achieve simultaneous A/D and D/A conversions of current, voltage, command and triggering signal for up to eight amplifiers. Custom-written Igor-based programs were used to operate the recording system and perform online and offline data analysis. Motorized manipulators (Lugis & Neumann Feinmechanik and Elektrotechnik) were custom-improved in stability to improve morphological recovery of axonal arborization of the recorded interneurons. More than 85% of recorded interneurons had their axonal arborization well-recovered and could be unambiguously classified into anatomical groups. These interneurons were included in the analysis. Neurons located in the same and neighboring columns were targeted by referring their relative locations to the barrels (if barrel cortical slices were used)[57], and/or more often to the characteristic clusters of ~10–20 closely packed large L5 pyramidal neurons located just inside of the columnar borders[52,58]. As no difference was found in general interneuronal circuit organization between the sensory and motor cortices (**Supplementary Tables 3** and **4**), the data were pooled in analysis. The presynaptic single action potential–evoked uIPSCs or uIPSPs in >3-week-old cortical neurons are highly reliable and often show no transmission failure[59,60]. Thus, inhibitory synaptic connections could be unambiguously identified after online monitoring of the average responses of short latency uIPSPs for ≥50 episodes. Unless otherwise specified, IPSCs and IPSPs were measured with membrane potentials of postsynaptic cells clamped or held at −55 mV and −55 ± 3 mV, respectively. Recording traces shown were averages of 50–200 consecutive episodes and the averages were also used to calculate the basic properties and kinetics of evoked uIPSCs and uIPSPs, such as synaptic latency, 10–90% rise time and decay time constant. Given that interneurons in acute slices seldom fired spontaneous action potentials, to achieve the maximal or near maximal suppression of dendritic complex spikes in L5 pyramidal neurons, we injected continuous depolarizing currents to induce tonic firing at ~5–15 Hz in L2/3 interneurons (**Fig. 7**). We then injected short depolarizing pulses at ~7–10 Hz in SBCs and ENGCs to evoke action potentials. The action potentials in SBCs blocked and those in ENGCs synchronized (to the same ~7–10 Hz) the firing in their connecting L2/3 interneurons (**Fig. 7**). Because the interaction of chemical and electric synapses is both necessary and effective in inducing stable firing synchronization in interneuronal networks[36,37], the mutual chemically and electrically connected ENGC and L2/3 interneuron pairs, the predominant connection configuration of the neurons (**Supplementary Fig. 3**), were selected to carry out the experiment in **Figure 7**.

Statistical analysis. Statistical results were reported as mean ± s.e.m. The sample size (n) represents the number of neurons, unless otherwise indicated. Statistical significances of the means ($P \leq 0.05$, two sides) were determined using Wilcoxon and ANOVA, Mann-Whitney rank sum nonparametric or χ^2 tests for paired and unpaired samples, respectively.

51. Huang, Z.J., Di Cristo, G. & Ango, F. Development of GABA innervation in the cerebral and cerebellar cortices. *Nat. Rev. Neurosci.* **8**, 673–686 (2007).
52. Zhu, J.J. Maturation of layer 5 neocortical pyramidal neurons: amplifying salient layer 1 and layer 4 inputs by Ca^{2+} action potentials in adult rat tuft dendrites. *J. Physiol. (Lond.)* **526**, 571–587 (2000).

53. Kielland, A. *et al.* Activity patterns govern synapse-specific AMPA-R trafficking between deliverable and synaptic pools. *Neuron* **62**, 84–101 (2009).
54. Shepherd, G.M., Stepanyants, A., Bureau, I., Chklovskii, D. & Svoboda, K. Geometric and functional organization of cortical circuits. *Nat. Neurosci.* **8**, 782–790 (2005).
55. Peters, A., Palay, S.L. & Webster, H.d. *The Fine Structure of the Nervous System: Neurons and their Supporting Cells*, 3rd edn. (Oxford University Press, 1991).
56. Margrie, T.W., Brecht, M. & Sakmann, B. *In vivo*, low-resistance, whole-cell recordings from neurons in the anaesthetized and awake mammalian brain. *Pflugers Arch.* **444**, 491–498 (2002).
57. Agmon, A. & Connors, B.W. Thalamocortical responses of mouse somatosensory (barrel) cortex *in vitro*. *Neuroscience* **41**, 365–379 (1991).
58. Ito, M. Simultaneous visualization of cortical barrels and horseradish peroxidase-injected layer 5b vibrissa neurones in the rat. *J. Physiol. (Lond.)* **454**, 247–265 (1992).
59. Tamás, G., Szabadics, J. & Somogyi, P. Cell type– and subcellular position–dependent summation of unitary postsynaptic potentials in neocortical neurons. *J. Neurosci.* **22**, 740–747 (2002).
60. Szabadics, J., Tamas, G. & Soltesz, I. Different transmitter transients underlie presynaptic cell type specificity of $GABA_{A,slow}$ and $GABA_{A,fast}$. *Proc. Natl. Acad. Sci. USA* **104**, 14831–14836 (2007).

doi:10.1038/nn.3305

Corrigendum: The organization of two new cortical interneuronal circuits

Xiaolong Jiang, Guangfu Wang, Alice J Lee, Ruth L Stornetta & J Julius Zhu
***Nat. Neurosci.* 16, 210–218 (2013); published online 13 January 2013; corrected after print 3 March 2013**

In the version of this article initially published, in Figure 8a under L1 Spontaneous, the last 400 ms of trace 4 was a duplicate of trace 3; for Figure 8c, the legend referred to a scale bar of 2 mV instead of 4 mV; in Figure 8e, incidence on the *y* axis was plotted in units of 0–0.8 Hz instead of 0–4%; and in Figure 7b the insets were not described. The insets show the sequences of soma/axon–dendrite–soma/axon-initiated events in the dendritic complex spikes at a timescale expanded by a factor of 2.5, with arrows indicating the timing of initiation of the dendritic slow potentials and second somatic action potentials. The errors have been corrected in the HTML and PDF versions of the article.